Self-Organized, Rodlike, Micrometer-Scale Microstructure of $Tb_3Sc_2Al_3O_{12}$−$TbScO_3$:Pr Eutectic

Dorota A. Pawlak,*[,†] Katarzyna Kolodziejak,[†] Sebastian Turczynski,[†,‡] Jaroslaw Kisielewski,[†] Krzysztof Rożniatowski,[§] Ryszard Diduszko,[†] Marcin Kaczkan,[||] and Michał Malinowski[||]

Institute of Electronic Materials Technology, ul. Wolczynska 133, 01-919 Warsaw, Poland, Institute of Materials Science and Engineering, Technical University of Lodz, ul. Stefanowskiego 1/15, 90-924 Lodz, Poland, Materials Science Department, Warsaw University of Technology, ul. Wołoska 141, 02-507 Warsaw, Poland, and Institute of Microelectronics and Optoelectronics, Warsaw University of Technology, ul. Koszykowa 75, 00-662 Warsaw, Poland

Received January 19, 2006. Revised Manuscript Received March 15, 2006

The self-organized rodlike microstructure of terbium-scandium-aluminum garnet−terbium-scandium perovskite, $Tb_3Sc_2Al_3O_{12}$−$TbScO_3$, eutectic crystals has been studied. The growth of the eutectic by the micro-pulling down method is presented. The obtained self-organized dielectric microstructure is made of perovskite fibers embedded in a garnet phase matrix. The crystal quality of both phases is confirmed by the structural analysis. Both phases can be etched away, depending on the composition, leaving a pseudo-hexagonally packed dielectric array of pillars or an array of pseudo-hexagonally packed holes in dielectric material. Both structures can be filled with metal or another material and, hence, have possible metamaterials or photonic crystals applications.

Introduction

In recent years, two different types of material are being developed in the area of photonics: photonic band gap materials[1−4] (photonic crystals) and metamaterials.[5−12] In photonic crystals, the wavelength of the light has to be comparable to the periodicity of the structure, to exhibit a photonic band gap effect. In metamaterials, on the other hand, the wavelength should be much bigger than the structuring of the matter since only the effective properties such as effective permittivity and permeability are important (diffraction should not take part in metamaterials). There are many sophisticated methods for obtaining these two types of materials. But they could also be obtained by self-organization.

In this paper a very promising method for growth of self-organized micro- and nanostructures is presented, for different types of light manipulation, based on directional solidification of eutectics. The eutectic is characterized by the formation of two unmixable crystals from a completely mixable melt. Metal−metal eutectics have been studied for many years, due to their excellent mechanical properties. Recently, oxide−oxide eutectics have also been studied, due to their excellent flexural strength and creep resistance at high temperature.[13−16] Oxide−oxide eutectics were lately also

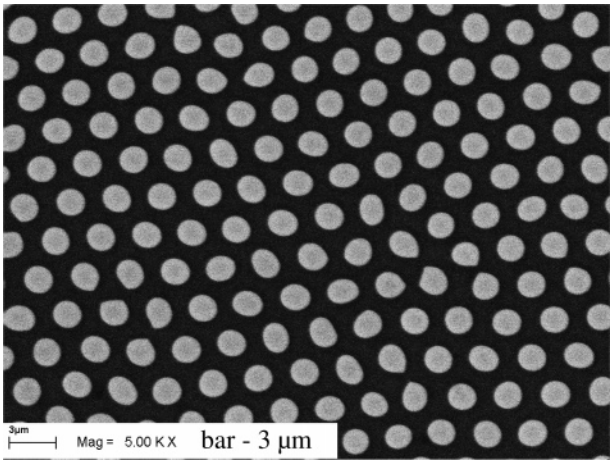

Figure 1. Self-organized pseudo-hexagonally packed $Tb_3Sc_2Al_3O_{12}$−$TbScO_3$ eutectic microstructure: cross-section (the perovskite phase is gray and the garnet phase is black). The contrast is generated by the different phases relative to their average atomic number.

* Corresponding author. E-mail: Dorota.Pawlak@itme.edu.pl. Tel.: +48 22 8349949.
† Institute of Electronic Materials Technology.
‡ Institute of Materials Science and Engineering, Lodz Technical University.
§ Materials Science Department, Warsaw University of Technology.
|| Institute of Microelectronics and Optoelectronics, Warsaw University of Technology.

(1) John, S. *Phys. Rev. Lett.* **1987**, *58*, 2486.
(2) Yablonowitch, E. *Phys. Rev. Lett.* **1987**, *58*, 2059.
(3) Joannopoulos, J. D.; Villeneuve, P. R.; Fan, S. *Nature* **1997**, *386*, 143.
(4) Von Blaaderen, A. *Science* **1998**, *282*, 887.
(5) Pendry, J. B. *Phys. Rev. Lett.* **2000**, *85*, 3966.
(6) Shelby, R.; Smith, D. R.; Schultz, S. *Science* **2001**, *292*, 77.
(7) Linden, S.; Enkrich, C.; Wegener, M.; Zhou, J.; Koschny, T.; Soukoulis, C. M. *Science* **2004**, *306*, 1351.
(8) Yen, T. J.; Padilla, W. J.; Fang, N.; Vier, D. C.; Smith, D. R.; Pendry, J. B.; Basov, D. N.; Zhang, X. *Science* **2004**, *303*, 1494.
(9) Pendry, J. B. *Science* **2004**, *306*, 1353.
(10) Fang, N.; Lee, H.; Sun, Ch.; Zhang, X. *Science* **2005**, *308*, 534.
(11) Smith, D. R.; Pendry, J. B.; Wiltshire, M. C. K. *Science* **2004**, *305*, 788.
(12) Wiltshire, M. C. K.; Pendry, J. B.; Young, I. R.; Larkman, D. J.; Gilderdale, D. J.; Hajnal, J. V. *Science* **2001**, *291*, 849.
(13) Waku, Y.; Nakagawa, N.; Wakamoto, T.; Ohtsubo, H.; Shimizu, K.; Kohtoku, Y. *Nature* **1997**, *389*, 49.
(14) Lee, J. H.; Yoshikawa, A.; Durbin, S. D.; Yoon, D. H.; Fukuda, T.; Waku, Y. *J. Cryst. Growth* **2001**, *222*, 791.
(15) Lee, J. H.; Yoshikawa, A.; Kaiden, H.; Lebbou, K.; Fukuda, T.; Yoon, D. H.; Waku, Y. *J. Cryst. Growth* **2001**, *231*, 179.
(16) Nakagawa, N.; Ohtsubo, H.; Mitani, A.; Shimizu, K.; Waku, Y. *J. Eur. Ceram. Soc.* **2005**, *25*, 1251.

10.1021/cm060136h CCC: $33.50
Published on Web 04/08/2006

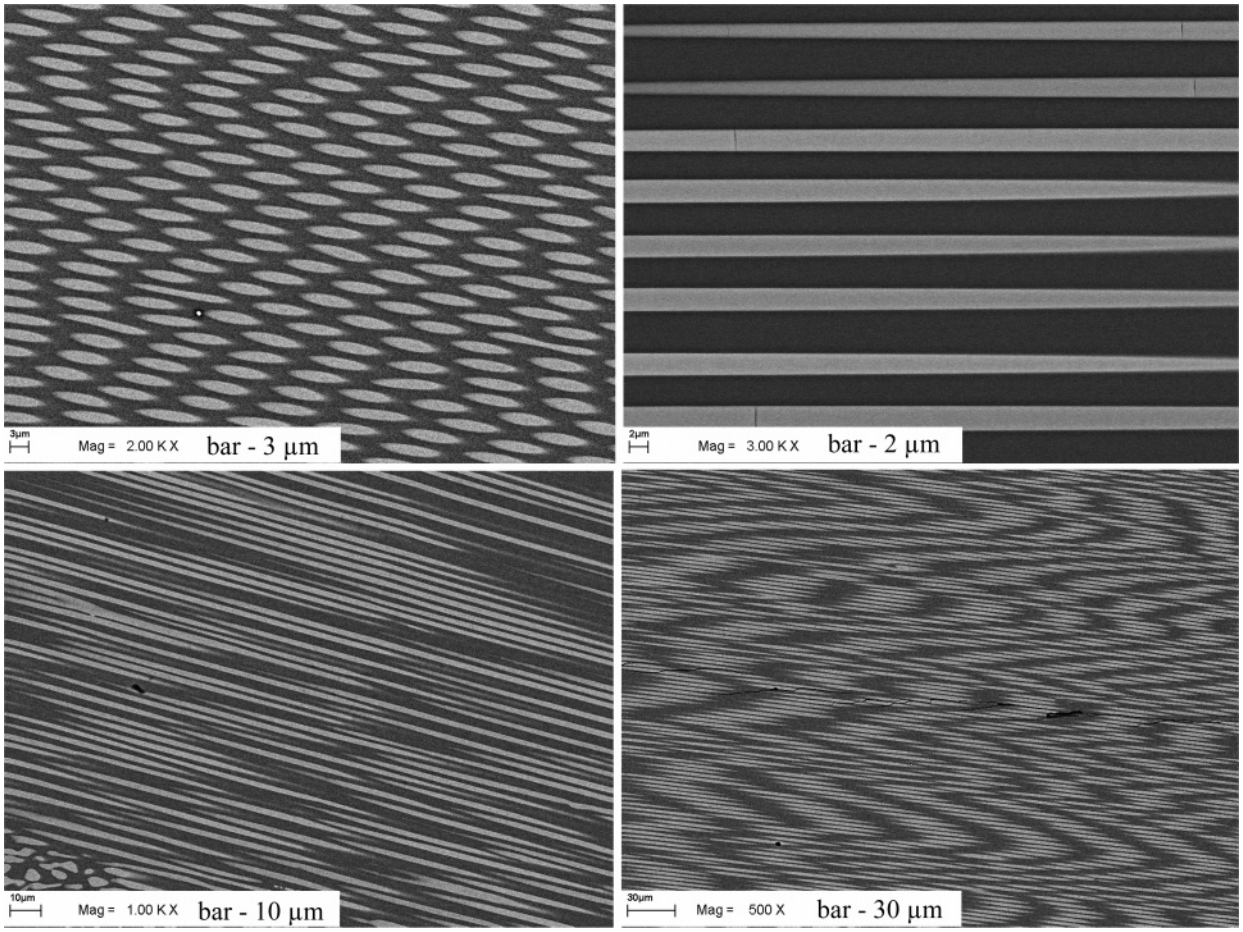

Figure 2. Section of the eutectic parallel to the growth direction, presenting the microrods.

identified by two groups as materials which could act as photonic crystals.[17,18] The eutectic reaction is nonvariant for binary eutectics. It represents a coupled growth of two phases from a binary liquid.[19] During cooperative growth, the alpha phase rejects B atoms and the beta phase rejects A atoms.[20] As Hecht et al.[19] states: "Coupled growth leads to a periodic concentration profile in the liquid close to the interface that decays in direction perpendicular to the interface much faster than in the single phases solidification." Depending on different factors, such as the entropy of melting of both phases, eutectics can form different micro- and nanostructures, classified by Hunt and Jackson: (i) nonfaceted−nonfaceted, when both phases have low entropies of melting, forming regular structure; (ii) nonfaceted−faceted, where one phase has low and one has high entropy of melting, forming irregular or complex microstructures; and (iii) faceted−faceted, where both phases have high entropies of melting, forming independent crystals.[21] The eutectic microstructure can exhibit many geometrical forms. It can be regular-lammelar, regular-rodlike, irregular, complex regular, quasi-regular, broken-lamellar, spiral, and globular. The most interesting from the point of view of photonic crystals would be the microstructures with regular shapes, i.e., lamellar and rodlike shapes. But for metamaterials applications the other shapes could also be of interest, for example, the percolated

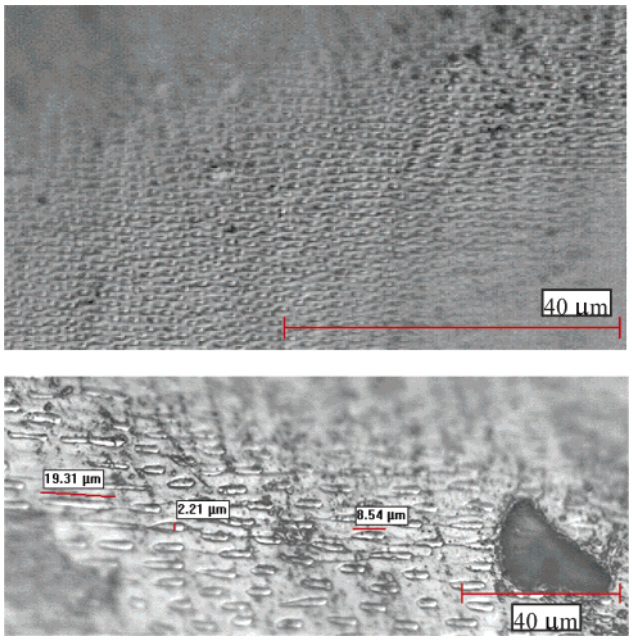

Figure 3. Surface of the eutectic fibers also indicates the eutectic structure. Images from the optical microscope with Nomarski contrast, magnification ×500.

(17) Pawlak, D. A.; Lerondel, G.; Dmytruk, I.; Kagamitani, Y.; Durbin, S.; Fukuda, T. *J. Appl. Phys.* **2002**, *91*, 9731.
(18) Merino, R. I.; Pena, J. I.; Larrea, A.; de la Fuente, G. F.; Orera, V. M. *Recent Res. Dev. Mater. Sci.* **2003**, *4*, 1.
(19) Hecht, U.; Granasy, L.; Pusztai, T.; Bottger, B.; Apel, M.; Witusiewicz, V.; Ratke, L.; De Wilde, J.; Froyen, L.; Camel, D.; Drevet, B.; Faivre, G.; Fries, S. G.; Legendre, B.; Rex, S. *Mater. Sci. Eng.* **2004**, *R46*, 1.
(20) Ashbrook, R. L. *J. Am. Ceram. Soc.* **1977**, *60*, 428.
(21) Hunt, J. D.; Jackson, K. A. *Trans. AIME* **1966**, *236*, 843.

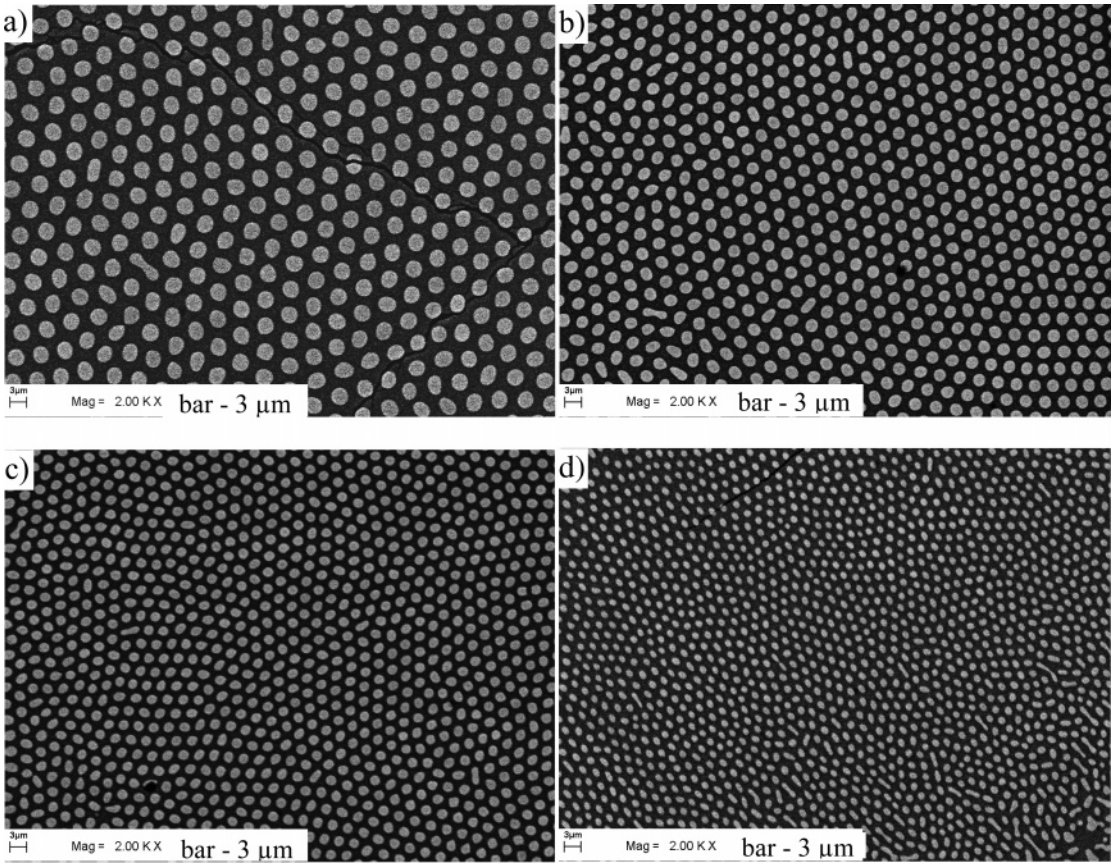

Figure 4. Change in the size of the microstructure of the binary eutectic $Tb_3Sc_2Al_3O_{12}-TbScO_3$ grown with different pulling rates: (a) 0.15, (b) 0.3, (c) 0.45, and (d) 1 mm/min.

structures (for giant dielectric constant[22]) or the spiral one for chiral metamaterials. The globular shape, which could find application in invisible materials[23] or in plasmon tunable materials (if the structure were metallodielectric) could also be interesting.[24] There are many methods for growing eutectics, such as laser floating zone (LFZ), the Edge-Defined Film-Fed-Growth technique, the Bridgman method, and the micro-pulling down method. The micro-pulling down method[25] was originally invented for the growth of single-crystal fibers but it is perfectly suited for the directional growth of eutectics.[14,15] In this paper we explore the utility of the micro-pulling down method for growth of self-organized microstructures of rodlike shape, using the terbium-scandium-aluminum garnet−terbium-scandium perovskite eutectic as an example. When only the minimum interface controlling the microstructure is taken into account, then the rodlike pattern is expected for a volume fraction of one of the phases $\leq 1/\pi$.[20,26]

Experimental Section

Crystal Growth. The micro-pulling down method was invented in Japan, originally for growth of single-crystal fibers.[25,27−29] The growth of oxide−oxide eutectics for the high-strength materials has already been reported.[14,15,30] High-purity oxide powders (99.995%), Tb_4O_7, Sc_2O_3, Al_2O_3, and Pr_6O_{11} were used as starting materials. The oxides were mixed with ethanol in alumina mortar and then dried. In the micro-pulling down method we have a crucible with a die at the bottom in which there is a centrally placed nozzle. The raw materials are melted in the crucible. The melt passes through the nozzle and is touched with the seed crystal, and the crystal is pulled down. The scheme of the thermal system used for micro-pulling down, as well as the growth conditions, will be described elsewhere.[31] The crystals grown were seeded with a ⟨111⟩ $Y_3Al_5O_{12}$ single crystal.

A fully aligned eutectic structure can only be obtained when the crystal/melt interface is flat. The other necessary conditions are as follows: steep temperature gradient, slow growth rate, and absence of convection.[20,32] All these conditions can be fulfilled by the micro-pulling down method.

The individual phases have been identified by combining the powder X-ray diffraction and energy dispersive spectroscopy.

Some samples were etched in phosphoric acid, H_3PO_4 85% cz.d.a. diluted with water 1:1.

Quantitative Analysis of the Microstructure. All the geometrical parameters were calculated from the scanning electron

(22) Pecharroman, C.; Esteban-Betegon, F.; Bartolome, J. F.; Lopez-Esteban, S.; Moya, J. S. *Adv. Mater.* **2001**, *13*, 1541.
(23) Garcia de Abajo, F. J.; Gomez-Santos, G.; Blanco, L. A.; Borisov, A. G.; Shabanov, S. V. *Phys. Rev. Lett.* **2005**, *95*, 067403.
(24) Riikonen, S.; Romero, I.; Garcia de Abajo, F. J. *Phys. Rev. B* **2005**, *71*, 235104.
(25) Yoon, D. H.; Yonenaga, I.; Ohnishi, N.; Fukuda, T. *J. Cryst. Growth* **1994**, *142*, 339.
(26) Hogan, L. M.; Kraft, R. W.; Lemkey, F. D. In *Advances in Materials Research*; Helman, H., Ed.; Wiley-Interscience: New York, 1971; Vol. 5, pp 83−216.
(27) Yu, Y. M.; Chani, V. I.; Shimamura, K.; Inaba, K.; Fukuda, T. *J. Cryst. Growth* **1997**, *177*, 74.
(28) Pawlak D. A.; Kagamitani, Y.; Yoshikawa, A.; Wozniak, K.; Sato, H.; Machida, H.; Fukuda T. *J. Cryst. Growth* **2001**, *226*, 341.
(29) Chani, V. I.; Yoshikawa, A.; Machida, H.; Fukuda T. *J. Cryst. Growth* **2000**, *212*, 469.
(30) Yoshikawa, A.; Hasegawa, K.; Lee, J. H.; Durbin, S. D.; Epelbaum, B. M.; Yoon, D. H.; Fukuda, T.; Waku, Y. *J. Cryst. Growth* **2000**, *218*, 67.
(31) Kolodziejak, K.; Turczynski, S.; Diduszko, R.; Klimek, L.; Pawlak, D. A. To be published.
(32) Mollard, F. R.; Flemings, M. C. *Trans AIME* **1967**, *10*, 1534.

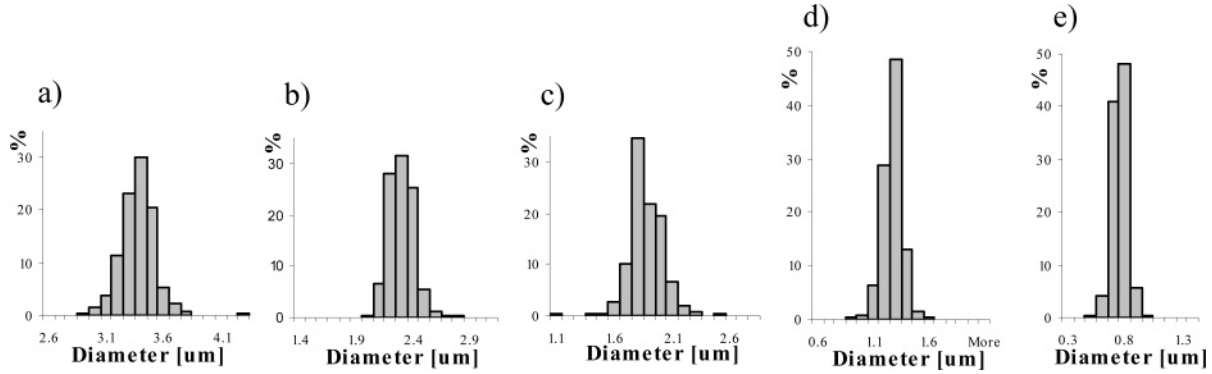

Figure 5. Microfiber diameter distribution for eutectics grown with different pulling rates: (a) 0.15, (b) 0.3, (c) 0.45, (d) 1, and (e) 4 mm/ min.

Table 1. Quantitative Analysis of the Size and Shape of the $Tb_3Sc_2Al_3O_{12}$−$TbScO_3$ Eutectic Microstructure

crystal number	p.r. (mm/min)	$\langle d \rangle$ (μm)	$\langle A \rangle$ (μm^2)	$\langle p \rangle$ (μm)	$\langle pC \rangle$ (μm)	$\langle V_V \rangle$ (%)
1	0.15	3.3 (0.05)	8.6 (0.11)	11.4 (0.10)	11.4 (0.09)	33.4
2	0.30	2.2 (0.04)	3.9 (0.09)	7.6 (0.06)	7.4 (0.06)	32.8
3	0.45	1.8 (0.07)	2.7 (0.13)	6.4 (0.11)	6.2 (0.10)	30.1
4	1.00	1.2 (0.07)	1.2 (0.13)	4.3 (0.09)	4.2 (0.08)	23.9
5	4	0.7 (0.08)	0.4 (0.15)	2.5 (0.10)	2.4 (0.10)	27.1

[a] p.r., crystal pulling rate; $\langle d \rangle$, mean diameter of the microfiber; $\langle A \rangle$, mean area of the cross section of the microfiber; $\langle p \rangle$, mean perimeter of the cross section of the microfiber; $\langle pC \rangle$, mean Cauchy perimeter of the cross section of the microfiber; $\langle V_V \rangle$, volume fraction of perovskite phase. The numbers in the brackets indicate the coefficient of variation CV. When CV is close to zero, all the parameters in the investigated area are similar.

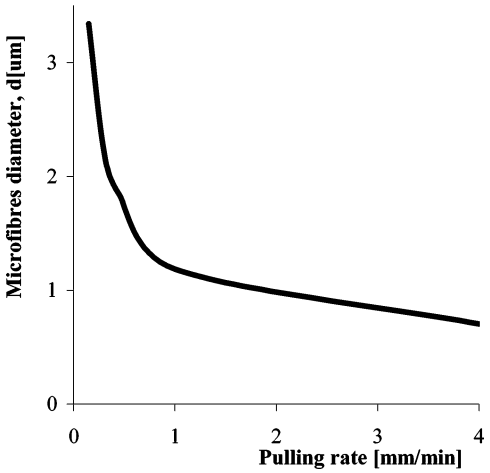

Figure 6. Dependence of the microrods diameter on the pulling of the eutectics $Tb_3Sc_2Al_3O_{12}$−$TbScO_3$.

microscope images by the MICROMETER program.[33] For each sample three images were chosen with a minimum of 300 investigated objects. The distribution of the microfibers was determined by the linear covariance and radial distribution functions. The first method consists of determining the linear covariance function, defined as the average probability that the plane $P + h$, formed by shifting a plane P which intersects a given particle, by a vector h, will also intersect this particle.[34] The covariance was determined along two directions: horizontal and vertical, with directional covariance functions denoted as $C(x)$ and $C(y)$. The distribution of microfibers was also described by the radial distribution function (RDF).[35] This could be defined as probability $H(r)$ of finding the particles at a specified radial distance, r. In a periodic structure, this function should have the form of a sequence of systematically repeated peaks. In a random or cluster-type structure, the number of peaks should decrease with increasing radius, whereas in a uniform structure, a practically constant value of the RDF should be seen.

Results and Discussion

Self-organized Rodlike Microstructure. The $Tb_3Sc_2Al_3O_{12}$−$TbScO_3$ eutectic with a volume ratio of V_{TSAG}:V_{TSP} = 2 has been chosen as the best composition for obtaining the rodlike microstructure. It was found that eutectic crystals with other compositions, such as V_{TSAG}:V_{TSP} = 4, and 3, did not contain enough of the perovskite phase and the eutectic was not present in all of the crystal; or when the pulling rate was high, it is in all of the crystal, but in the form of spider-like patterns. In the eutectic crystals containing a smaller amount of the garnet phase, like V_{TSAG}:V_{TSP} = 1, half as many dendrites of the perovskite phase are formed.[31] The possibility of obtaining a rodlike microstructure in a $Tb_3Sc_2Al_3O_{12}$−$TbScO_3$ off-eutectic has already been shown. During the growth of the single crystals of terbium-scandium-aluminum garnet, a small ca. 200 μm-wide outside layer is formed around the single crystal, which constitutes the $Tb_3Sc_2Al_3O_{12}$−$TbScO_3$ eutectic.[17] In this work the $Tb_3Sc_2Al_3O_{12}$−$TbScO_3$ eutectics doped with 5 at. % of praseodymium were grown by the micro-pulling down method in the form of rods with diameter 3 and 1.5 mm and length typically >10 cm. Praseodymium was added in order to investigate the spectroscopic properties of the eutectic microstructure in comparison with single crystals. The cross section of the rodlike self-organized microstructure of the investigated eutectic is shown in Figure 1. The fibers tend to pack hexagonally. The longitudinal section of the eutectics (parallel to the crystal growth direction) is shown in Figure 2. In almost all cases in the longitudinal section we see short pieces of microrods; long straight microrods are rarely found. The microrods usually tend to have sinusoidal or maybe even spiral shape, which implies that on the SEM micrograph of a cross section of the eutectic all the microrods have very similar diameters. (If the microrods were short, we would expect a micrograph of the microrods cross section to show microrods with many different diameters.) It could also be

(33) Wejrzanowski, T.; Bucki, J. J. *MICROMETER 0,99b − computer program for image analysis*. From Wejrzanowski, T. Computer based analysis of the microstructure of gradient materials. M.Sc. Thesis, Warsaw University of Technology, Warsaw, 2000.

(34) Susagna, F.; Yotte, S.; Riss, J.; Breysse, D.; Ghosh, S. *Proc. 6th Int. Conf. Stereol. Image Anal. Mater. Sci., Stermat* **2000**, 397.

(35) Hanisch, K. H.; Stoyan, D. *J. Microsc.* **1981**, *122*, 131.

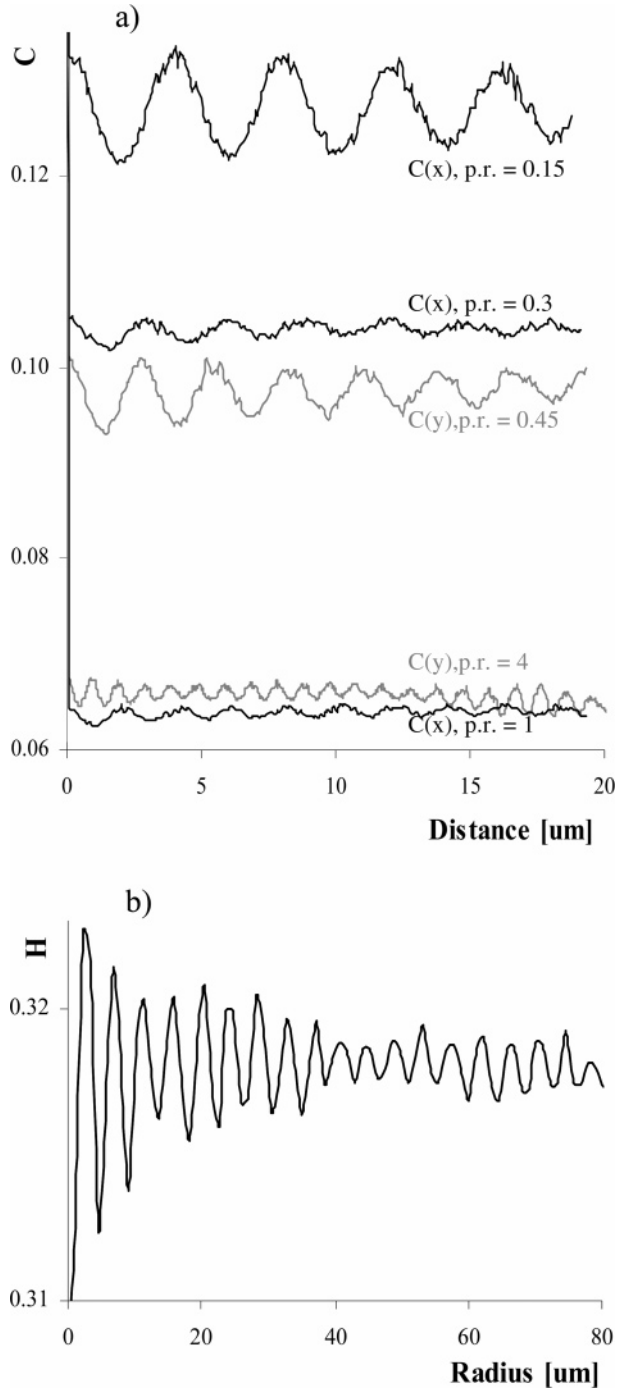

Figure 7. (a) Covariance function determined along the horizontal direction, $C(x)$, and in the vertical direction, $C(y)$, for the eutectics grown with the pulling rates 0.15, 0.3, 0.45, 1, and 4 mm/min. (b) An example of the radial distribution function for a sample grown with 0.15 mm/min pulling rate.

that we never succeed in cutting the crystal parallel to the microrods.

The eutectic microstructure is also seen on the surface of the grown eutectic fibers (Figure 3).

Dependence on the Pulling Rate. The terbium-scandium-aluminum garnet−terbium-scandium perovskite ($Tb_3Sc_2Al_3O_{12}$−$TbScO_3$, TSAG-TSP) eutectic doped with praseodymium has been grown with different pulling rates: 0.15, 0.3, 0.45, 1, and 4 mm/min. The diameter of the microrods decreases with increasing the pulling rate (see Figure 4). This ability to control the size of the microstructure with the pulling rate is important for potential applications.

The quantitative description of the microstructures has been performed using the MICROMETER 0,99b program.[33] All the parameters for each eutectic were calculated from three SEM micrographs containing a minimum of 300 data points (microrods, maximum 1400), and then the average parameters were calculated. These average parameters are shown in Table 1. In the investigated areas all the parameters are very similar to each other, as demonstrated by the coefficient of variation CV which is almost always very close to zero. The diameter of the microrods changes from 3.3 to 0.7 μm for pulling rates 0.15 and 4 mm/min, respectively. The distribution of microrod diameter of eutectics grown with different pulling rates is shown in Figure 5. In Figure 6 the dependence of the microrods diameter on the pulling rate of the $Tb_3Sc_2Al_3O_{12}$−$TbScO_3$ eutectics is shown. The area of the cross section of the microrods changes from 8.6 to 0.4 μm^2 for pulling rates 0.15 and 4 mm/min, respectively. The measured area is close to the one calculated using the measured diameter area, which indicates that the cross sections of the microrods are nearly circular. Slightly bigger differences are observed for the measured and calculated perimeter. The volume fraction of praseodymium perovskite phase generally decreases with the pulling rate, although for the highest pulling rate of 4 mm/min an increase is observed. This agrees with the fact that in all cases some dendrites of the perovskite phase are observed in addition to the eutectic phase. And at the higher pulling rate, many more dendrites of $TbScO_3$ are observed. The local ordering of the eutectic microstrucure is fairly high, as indicated by the linear covariance analysis (Figure 7a). The linear covariance analysis shows the probability of finding an object at some distance from a similar object (see Experimental Section); in a periodic structure, the linear covariance function should also be periodic (systematically repeated peaks). In Figure 7a the examples of linear covariance functions are shown for five different samples grown with different pulling rates (0.15, 0.3, 0.45, 1, and 4 mm/min) in either horizontal or vertical direction, $C(x)$ or $C(y)$. In these samples peaks are observed with strong periodicity in the range of $\geq$20 μm.

The distribution of microrods can also be represented by the radial distribution function (RDF),[35] the probability $H(r)$ of finding the particles at a specified radius, r. Again in a periodic structure, this function should itself be periodic. The peaks in the radial distribution function $H(r)$ show that the probability of finding an object is higher at certain radial distances. In Figure 7b the radial distribution function is shown for a sample grown with a pulling rate of 0.15 mm/min. Evidently, the sample is locally ordered within a radius of $\leq$80 μm.

Hybrid Structure. In the field of metamaterials, hybrid materials such as metallodielectric materials are sought.[23,24] To obtain metallodielectric materials from the oxide−oxide eutectic, one phase can be removed by etching and then the empty space can be filled with metal. The theoretical properties of similar plasmonic structures have already been reported[36]

(36) Garcia-Vidal, F. J.; Martin-Moreno, L.; Pendry, J. B. *J. Opt. A: Pure Appl. Opt.* **2005**, *7*, S97.

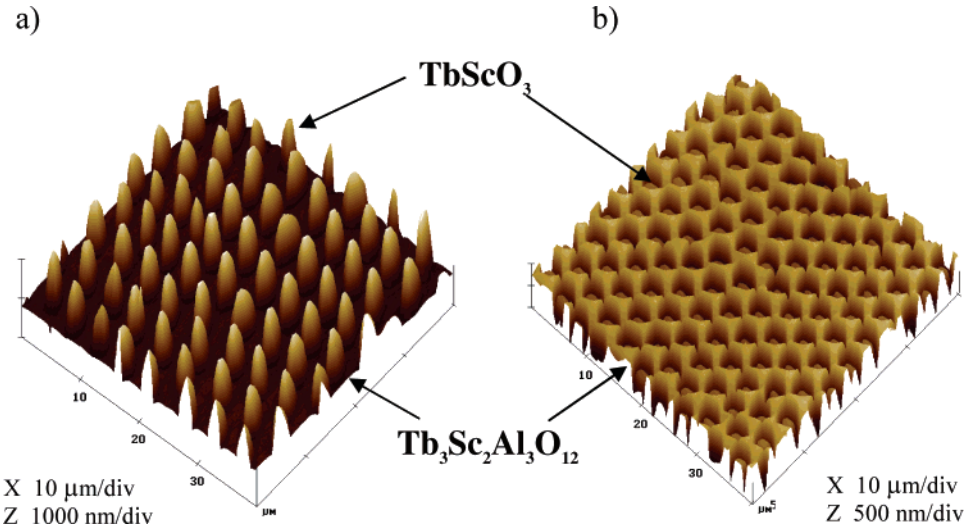

Figure 8. Atomic force micrographs of different microstructures obtained by etching one of the phases of $Tb_3Sc_2Al_3O_{12}$−$TbScO_3$ eutectic with phosphoric acid: (a) the array of pseudo-hexagonally packed $TbScO_3$ microfibers obtained when the garnet phase etched more rapidly; (b) the array of pseudo-hexagonally packed holes in a $Tb_3Sc_2Al_3O_{12}$ matrix obtained when the perovskite phase etched more rapidly.

Let us consider first the $Tb_3Sc_2Al_3O_{12}$−$TbScO_3$ off-eutectic, which exists only at the edge of the $Tb_3Sc_2Al_3O_{12}$ crystal. Following etching with phosphoric acid of such eutectic, the garnet phase is removed and an array of dielectric-perovskite pillars remain on the surface. This was already reported in ref 17, and the same results have been found in this work (Figure 8a). In this case both phases are etched, but garnet phase etches more rapidly.

Etching the $Tb_3Sc_2Al_3O_{12}$−$TbScO_3$ eutectic (which exists in the "fully eutectic" crystal) has the opposite effect: both garnet and perovskite phases are etched, but the etching rate for the perovskite is higher, resulting in a garnet matrix with an array of pseudo-hexagonally packed air holes (Figure 8b). Actually, the fastest etching takes place at the border between garnet and perovskite phases. After etching in boiling phosphoric acid for 5 min, an array of holes is seen in the garnet phase, but in these holes are still some remains of perovskite rods. Figure 9 shows the cross section of these perovskite microrods. The typical height of the microrods after etching for 5 min in boiling phosphoric acid is 1.2−1.5 μm. In Figure 9b the cross section of the array of holes embedded in the garnet matrix is shown. After 5 min boiling in phosphoric acid the holes still contain the remains of the perovskite fibers. The depth from the surface to the top of the remaining rods is ca. 250 nm, while the deepest part of the hole is ca. 1 μm. In Figure 9c the cross section through the deepest part of the hole is shown. After etching for 10 min, the remaining fibers are removed, and the depth of the hole is still 1 μm.

After the etching process, the empty space can be filled with metal. In this work the empty spaces were filled with aluminum deposited by evaporation in both microstructures represented by Figures 8a and 8b. In Figure 10a the array of $TbScO_3$ microfibers previously embedded in air (Figure 8a) and now embedded in aluminum is shown. Aluminum was deposited to a height of 250 nm. If the structure were completely filled in with metal, the unnecessary "bumps" of aluminum (in the case of the array of microfibers) could

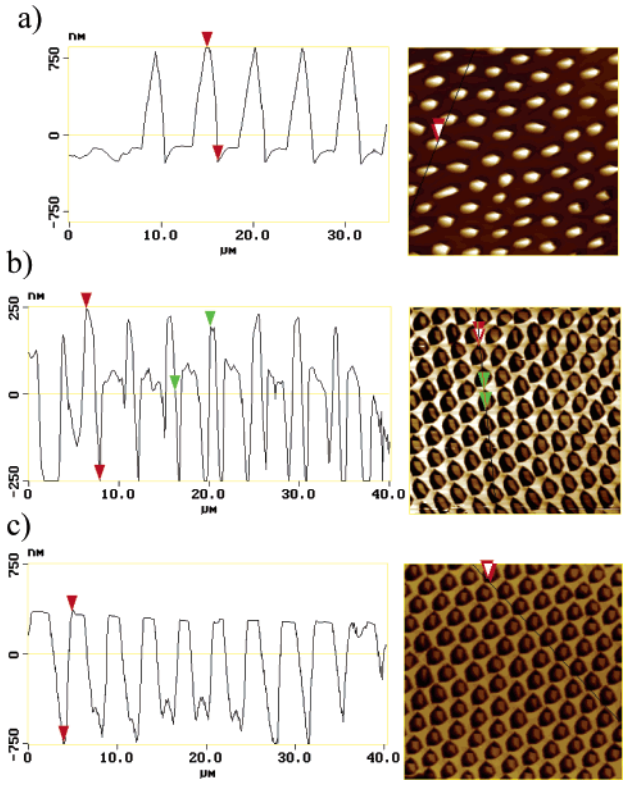

Figure 9. AFM images and the cross sections of different microstructures obtained by etching one of the phases of $Tb_3Sc_2Al_3O_{12}$−$TbScO_3$ eutectic with phosphoric acid: (a) the array of pseudo-hexagonally packed $TbScO_3$ microfibers; (b) the array of pseudo-hexagonally packed holes in a $Tb_3Sc_2Al_3O_{12}$ matrix and the cross section through the center of the holes, which includes residual $TbScO_3$ microrods; (c) the array of pseudo-hexagonally packed holes in a $Tb_3Sc_2Al_3O_{12}$ matrix and the cross section through the deepest part of the holes.

be polished away. In Figure 10b the array of holes (shown in Figure 8b) in the garnet matrix on which the aluminum was evaporated is shown. If the aluminum metal were polished away from the surface, one would see the structure of metal features embedded in the garnet matrix. Figure 10b reveals that, in the case of etching of the $Tb_3Sc_2Al_3O_{12}$−$TbScO_3$ eutectic, not only the perovskite but also the garnet

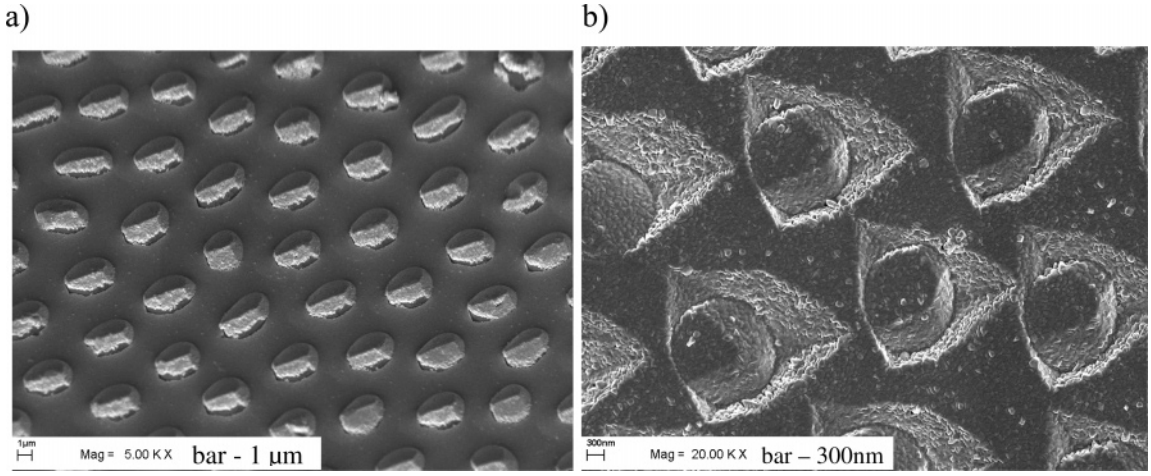

Figure 10. Microstructures obtained by etching one of the phases of the $Tb_3Sc_2Al_3O_{12}-TbScO_3$ eutectic with phosphoric acid, followed by deposition of evaporated aluminum to a height of 250 nm: (a) the array of $TbScO_3$ microfibers; (b) the array of holes in the $Tb_3Sc_2Al_3O_{12}$ matrix.

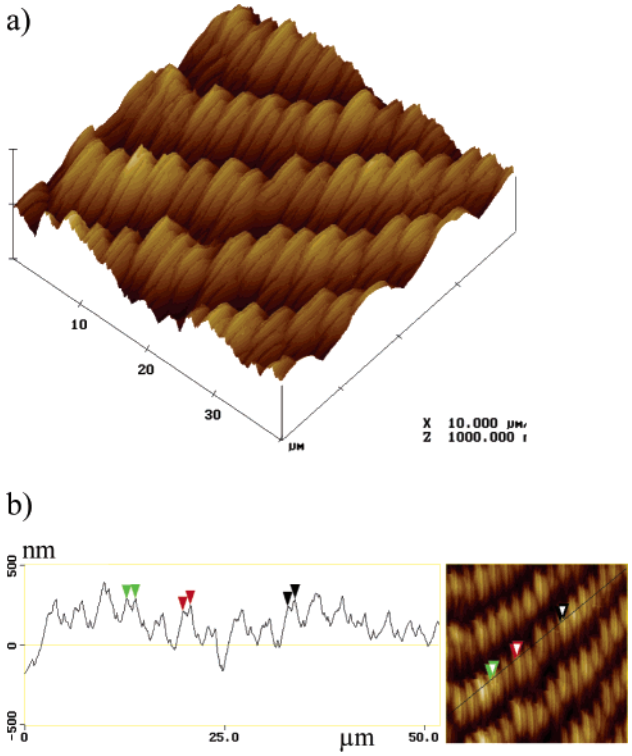

Figure 11. AFM image of the longitudinal section of the $Tb_3Sc_2Al_3O_{12}-TbScO_3$ eutectic after etching away one of the phases with phosphoric acid for 5 min.

phase (the matrix) is etched. It shows triangular shapes because the garnet phase grows in the ⟨111⟩ direction (this has been confirmed by single-crystal XRD). In the ⟨111⟩ direction in the garnet phase there is a $\bar{3}$ crystallographic axis.

Figure 11a shows an atomic force micrograph of the longitudinal section of the $Tb_3Sc_2Al_3O_{12}-TbScO_3$ eutectic following etching of one phase with phosphoric acid for 5 min. Figure 11b shows the cross section of the structure shown in Figure 11a. It is rather difficult to interpret these images. In the case of the $Tb_3Sc_2Al_3O_{12}-TbScO_3$ eutectic, it should be the perovskite phase which mainly gets etched away and does appear to be the case for the cross section of the eutectic.

Spectroscopic Properties. In Figure 12c the global emission spectrum of $Tb_3Sc_2Al_3O_{12}-TbScO_3$ eutectic doped with Pr ions is shown, in the range from 480 to 900 nm. It is compared with the emission of pure $Tb_3Sc_2Al_3O_{12}-TbScO_3$ eutectic (Figure 12b) and the emission of a $Tb_3Sc_2Al_3O_{12}$ single crystal (Figure 12a). The luminescence corresponding to four different transitions of Tb^{3+} is observed. The emission bands in the range 480−510 nm correspond to $^5D_4 \rightarrow {}^7F_6$ transition; 530−560 nm corresponds to the $^5D_4 \rightarrow {}^7F_5$ transition; and in the 575−635 nm range $^5D_4 \rightarrow {}^7F_4$ and $^5D_4 \rightarrow {}^7F_3$ transitions are observed. The luminescence associated with these transitions exists for other garnet crystals containing terbium ion, for example, $Y_3Al_5O_{12}$:Tb[37] and $Tb_xA_{3-x}Al_5O_{12}$ (A = Yb, Y).[38] In Figure 12 the luminescence of the single crystal of $Tb_3Sc_2Al_3O_{12}$ obtained in this work is shown. No literature data could be found on the emission of a $TbScO_3$ single crystal. For the eutectic, there are emission peaks which are not present in the pure garnet phase, such as the peak at 613 nm. There is no difference in the shape of the pure eutectic and the eutectic doped with 5 at. % of praseodymium ions. A more detailed description of the spectroscopic properties of the investigated eutectics will be presented elsewhere.[39]

Conclusion

The growth of self-organized rodlike microstructure of terbium-scandium-aluminum garnet−terbium-scandium perovskite eutectic have been obtained by the micro-pulling down method. The microrods of the perovskite phase are packed pseudo-hexagonally in the garnet matrix. The diameter of the microrods can be controlled by the pulling rate. Depending on the composition, one of the two phases can

(37) Mazur, P.; Hreniak, D.; Niittykoski, J.; Strek, W.; Hölsa, J. To be published in *Mater. Sci.*
(38) Nikl, M.; Solovieva, N.; Dusek, M.; Yoshikawa, A.; Kagamitani, Y.; Fukuda, T. *J. Ceram. Process. Res.* **2003**, *4*, 112.
(39) Kaczkan, M.; Malinowski, M.; Klimczuk, T.; Pawlak, D. A.; Kolodziejak, K.; Piersa, M. To be published.

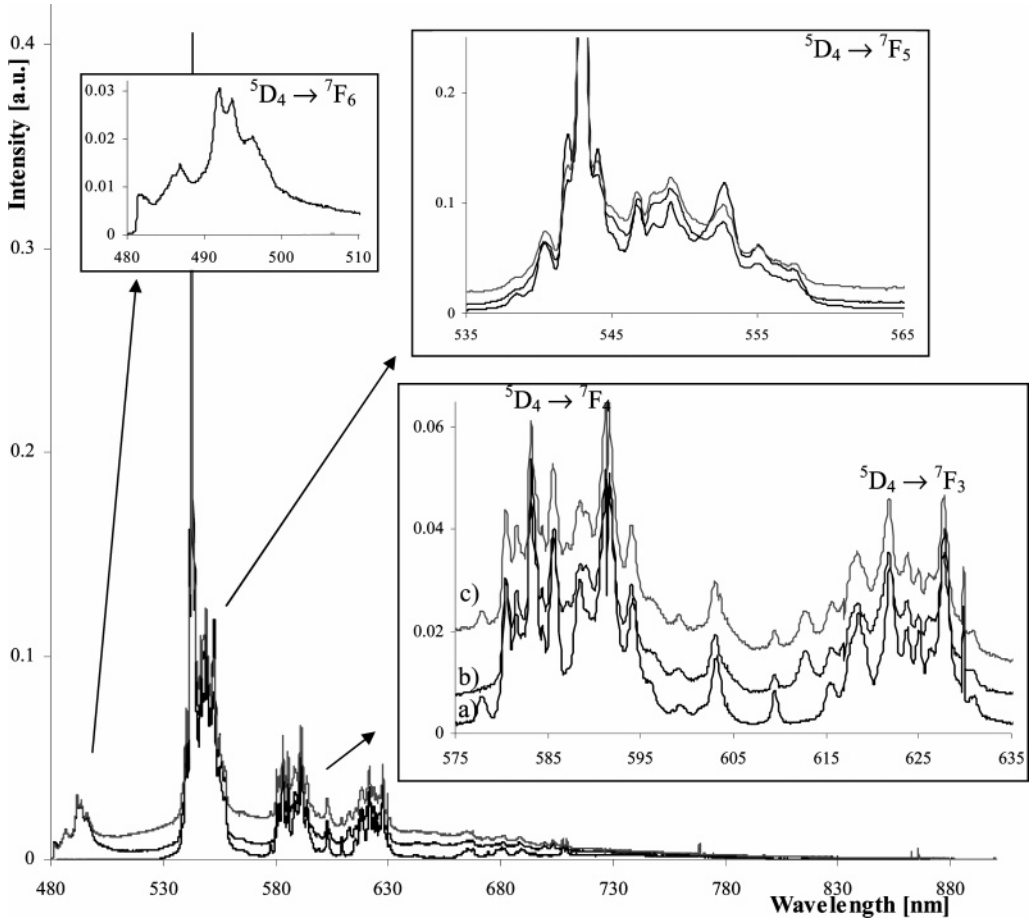

Figure 12. Emission spectra of (a) $Tb_3Sc_2Al_3O_{12}$ single crystal, black line; (b) $Tb_3Sc_2Al_3O_{12}$−$TbScO_3$ eutectic, dark gray line; (c) $Tb_3Sc_2Al_3O_{12}$−$TbScO_3$ eutectic doped with 5 at. % Pr, light gray line. Inset I: Enlargement of emission spectra of $Tb_3Sc_2Al_3O_{12}$−$TbScO_3$ eutectic in the region 480−500 nm. Inset II: Enlargement of emission spectra in the region 535−565 nm. Inset III: Enlargement of emission spectra in the region 575−635 nm.

be etched away with phosphoric acid. If the eutectic appears only at the edge of the $Tb_3Sc_2Al_3O_{12}$ crystal, then etching results in an array of dielectric microrods of the perovskite phase. When the $Tb_3Sc_2Al_3O_{12}$−$TbScO_3$ eutectic exists throughout the whole crystal volume, then etching gives the inverse structure, i.e., an array of holes embedded in the dielectric matrix made of garnet phase. Both types of structure can be filled with metal to give a metallodielectric material with potential applications in the field of metamaterials.

Acknowledgment. The authors thank the Ministry of Scientific Research and Information Technology of Poland for support of this work (Grant No. 4 T11B 015 24). The authors acknowledge the Network of Excellence, METAMORPHOSE (No. 500252). The authors also thank Mr. Teodorczyk for metal evaporation, Dr. R. Bożek from the Department of Physics, Warsaw University, for the possibility of AFM measurements, and Dr. Siân Howard (University of South Australia) for a critical reading of the manuscript.

CM060136H